NOTES AND CORRESPONDENCE

An Efficient Sound Source for Wide-Area RAFOS Navigation

T. ROSSBY

Graduate School of Oceanography, University of Rhode Island, Kingston, Rhode Island

J. ELLIS

Sparton of Canada, London, Ontario, Canada

D. C. WEBB

Webb Research Corporation, Falmouth, Massachusetts

2 February 1992 and 24 August 1992

ABSTRACT

To meet the expected need for wide-area acoustic navigation for Lagrangian studies of ocean circulation using RAFOS floats, a new and powerful sound source, a resonant pipe projector has been developed. It consists of a free-flooded open steel pipe with a ceramic–steel driver ring at its midsection. Conservatively demonstrated here at a source level of 195.5 dB re 1 μPa @ 1 m and with an energy conversion efficiency of 85% at resonance (260 Hz), useful operating ranges to 4000 km and beyond are possible, depending on ambient noise conditions. A successful 6-month accelerated test of the complete transducer system was recently completed near Bermuda.

1. Introduction

The interest expressed by the World Ocean Circulation Experiment (WOCE) community in using the RAFOS float technology (Rossby et al. 1986) for ocean circulation studies on the basin scale (e.g., WOCE 1989) stimulated a search for a sound-source transducer that would be able to insonify a larger region than the standard SOFAR float source so that wide-area navigation could be provided with a modest number of moored sources. The University of Rhode Island design goal was a 260-Hz (nominal) transducer capable of operating at 196 dB re 1 μPa @ 1 m, or about 20 dB more powerful than the source then in use. After a number of technical designs—including Helmholtz resonators, slotted cylinder, and flextensional transducers—were solicited and carefully reviewed, a proposal from Sparton of Canada (SOC) for a "resonant pipe projector" (RPP) was selected. The reasons for this choice were several, including the following. 1) The design was mechanically straightforward. 2) The concept was well known from earlier development work by the Defense Research Establishment (DREA), Dartmouth, Novia Scotia, and SOC (Lee 1974; Fanning et al. 1987). 3) The mechanical and electroacoustical properties of the transducer could be modeled very accurately using a finite-element analysis package called MAVART (Armstrong and McMahon 1984), and preliminary analysis indicated that the transducer would be highly efficient. 4) The transducer is free-flooding; hence, there are no pressure limitations. Its narrow bandwidth, approximately 3 Hz, was an inconvenience only in terms of tuning, not usage, since only 1.5 Hz was required. We give a brief technical description of the sound source and summarize the results from a half-year-long accelerated test of the prototype.

2. The sound-source transducer

a. Mechanical characteristics

The RPP is a free-flooded steel pipe open at both ends with a piezoelectric ceramic–steel composite driver ring around its midsection. The driver ring is prestressed into compression onto the steel pipe with fiberglass roving. When the ring is driven with an appropriate voltage, the resulting radial motion is effectively coupled to the pipe. The resulting pressure fluctuations generate a standing wave mode, since the pipe acts essentially as a half-wavelength resonator. Figure 1 is a schematic drawing of the transducer. The RPP is rolled from 0.64-cm-thick steel and is 1.793 m long and 0.559 m in diameter. Three mounting holes are

Corresponding author address: Dr. H. Thomas Rossby, Graduate School of Oceanography, University of Rhode Island, Narragansett Bay Campus, Narragansett, RI 02882-1197.

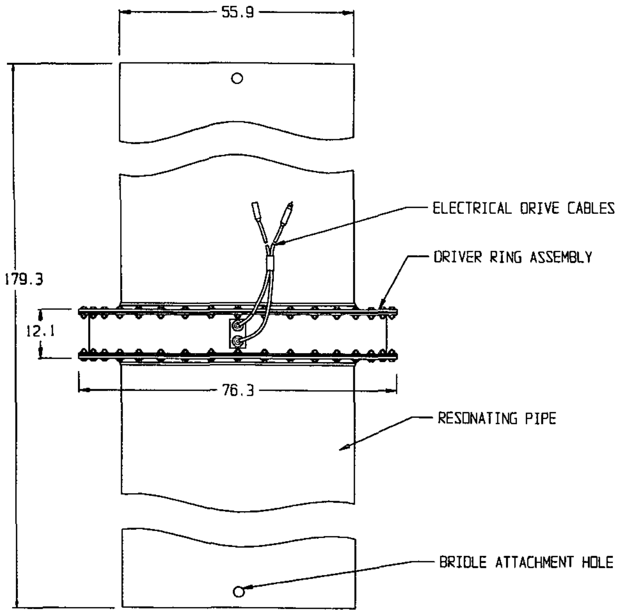

FIG. 1. Schematic drawing of the resonant pipe projector. The piezoelectric driver ring is prestressed into compression against the midsection of the pipe. It is encapsulated in a three-piece rubber boot assembly that is clamped together by the two sets of bolts. The pipe dimensions are 1.793 m long, 0.559 m diameter, and with a 0.64-cm wall thickness. It weighs 241 kg in air and 198 kg in water.

provided at each end of the pipe for the attachment of a mooring bridle. The piezoelectric transducer ring is covered with an oil-filled neoprene boot made up of three parts that are clamped together. The whole assembly is painted with epoxy paint. The driver ring is made up of electrically matched pairs of thickness-poled piezoelectric ceramic staves. Each pair of staves forms a ceramic element that is assembled alternately with tapered metal staves to form the driver ring. The metal staves provide electrical ground to one side of each ceramic stave. All pairs of staves are coupled in parallel. The signal bus wire and the ground return exit the pipe in a pair of 14-gauge conductor leads, which are terminated with Mecca Teledyne connectors. The RPP weighs 241 kg in air and 198 kg in water. Figure 2 is a photograph of the transducer during recovery after a 6-month accelerated test off Bermuda.

b. Electrical–acoustical properties

The susceptance and conductance of the RPP is shown in Fig. 3a. Particularly the conductance is highly frequency dependent, reflecting the narrow bandwidth of the transducer. The measured susceptance and conductance at the fundamental resonance frequency of 260 Hz are 0.55 and 0.18 mS, respectively. By the use of an inductor, the circuit can be tuned so that the drive voltage and current are in phase at resonance. The transmitting voltage response is shown in Fig. 3b, and at resonance is 136 dB re 1 μPa V^{-1} @ 1 m. The narrow bandwidth of the RPP is evident; the 3-dB points are only 3 Hz apart. This does not affect the performance of the RPP in operation since we require only 1.5 Hz, but it does mean that the length of the pipe must be determined very carefully to ensure that it is resonant at the speed of sound where the transducer will be deployed. This was done by measuring its transmitting voltage response (TVR) in saltwater (Bedford Basin, Novia Scotia) and then trimming the length of the pipe for the speed of sound in the SOFAR channel.

To achieve the desired 196 dB re 1 μPa source level, a drive voltage of 1000 V_{ac} is required. This is comfortably less than the 3500-V_{ac} voltage limit of the piezoelectric ceramic elements. The radiation pattern is uniform in the horizontal plane and doughnut shaped in the vertical (Fig. 4). The measured radiation pattern is also shown. The absence of the nodes along the axis is due to reverberation from the bottom and surface at

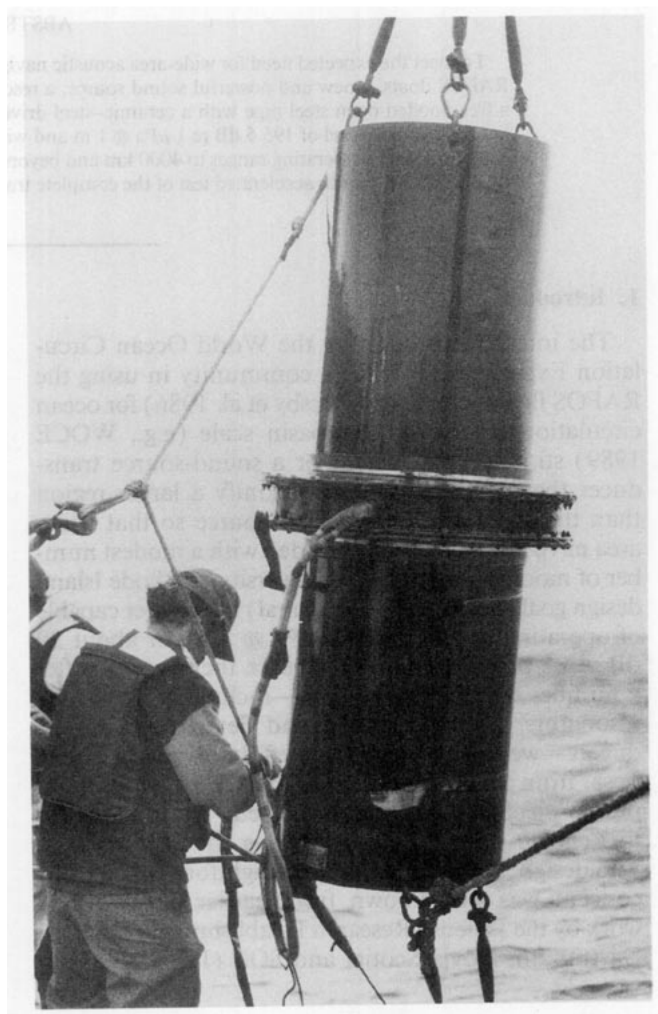

FIG. 2. Photograph of the resonant pipe projector (RPP) during recovery at the end of a 6-month accelerated test. There was no evidence of any corrosion on the pipe.

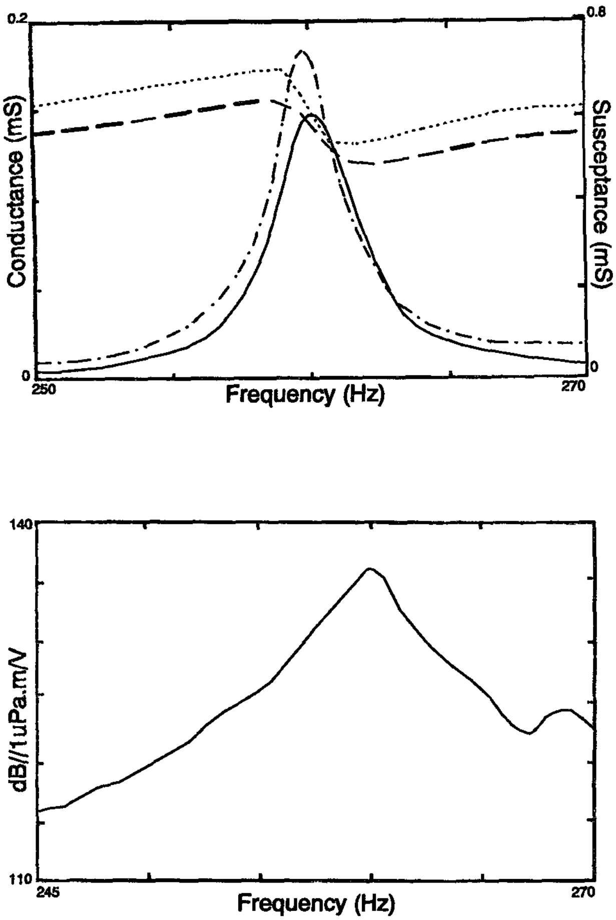

FIG. 3. (a) MAVART-predicted (solid line) and measured (dash-dot) conductance (mS), and MAVART-predicted (dashed) and measured (dotted) susceptance (mS) as a function of frequency in water. (b) Measured transmitting voltage response (TVR) as a function of frequency.

the test site. This horizontal beam forming provides a welcome 2.9-dB gain (MAVART-predicted value) over an equivalent omnidirectional radiator. At resonance the projector has an electroacoustic conversion efficiency of 85%, estimated from the integral of the MAVART-predicted sound intensity over the entire spherical radiating surface and comparing this to the electrical input power.

c. Sound-source electronics package

The transducer is driven by a separate electronics and power module supplied by Webb Research Corp (WRC). It is essentially the same as a standard SOFAR float without its transducer, but with a modified power amplifier to deliver about 200 W. It consists of a watertight 0.3-m o.d. aluminum pipe, 3.05 m long, with a 1.9-cm wall thickness, giving it a maximum operating pressure of 20 MPa (=2000 db). The transmitted signal consists of a frequency-modulated sweep of 80-s duration where the frequency is incremented linearly from 259.375 to 260.898 Hz in 2-s steps at each of which phase continuity is preserved. This is the standard FM SOFAR float signal that has been in use since 1975 (Webb 1977). The output stage consists of four power FETs (field effect transistors) in an H configuration driving a tuned primary winding. The secondary winding is parallel tuned to match the susceptance of the RPP at resonance. The electronics are controlled through a 20-mA current loop conforming to the SAIL (shipboard ASCII instrumentation loop) communications protocol. Parameters that can be set or examined include the clock, transmission schedule, acoustic power level, battery voltage, and internal gas pressure. Energy is provided from 24 packs of alkaline battery packs (each one consisting of 30 D cells), which are wired in parallel with diode protection. With 1.8 MJ per pack, the stored energy is sufficient for (24 × 1.8 MJ)/(80 s × 200 W) = 2700 signals. There is space in the 3-m tube for a total of 33 packs. In the field test described below, 540 signals were transmitted (180 × 3 per day).

The transducer is powered at 180 W electric or 940 V_{ac}. These measured values were obtained using a dummy load with a conductance and susceptance that closely matches the RPP at resonance. The sound pressure level can be estimated two ways. One is to use the measured voltage and the TVR curve in Fig. 3b (136 dB re 1 μPa/V @ 1 m). This leads to a sound pressure level of 195.5 dB re 1 μPa @ 1 m, or very

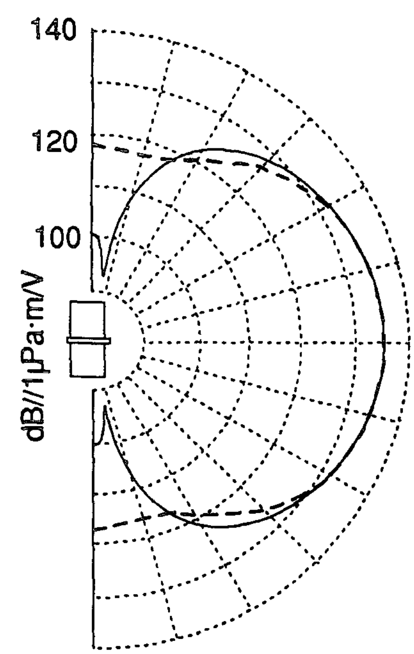

FIG. 4. Predicted (solid) and measured (dashed) radiation pattern in the vertical direction. Reverberation from the surface and bottom makes it impossible to resolve the axial nodes. The transducer has a computed gain of 2.9 dB in the horizontal relative to an omnidirectional radiator.

close to the design goal. The second approach is based on an energy budget. A 1-W omnidirectional radiator has a sound pressure level of 170.8 dB re 1 μPa @ 1 m. To this add 22.6 dB (180 W) and the 2.9-dB horizontal gain from Fig. 4 and subtract 0.7 dB for the 85% energy conversion efficiency of the transducer. The result is 195.6 dB re 1 μPa @ 1 m.

3. Operational considerations

The mooring design is shown schematically in Fig. 5. It follows procedures that have been developed and used very effectively at the Woods Hole Oceanographic Institution. Flotation is provided by 30 glass balls, mostly at the top. A UHF radio beacon and flasher housed in a glass ball to aid relocation at the surface is attached to the top of the mooring by means of a long tether. A similarly housed Argos beacon is attached as a relocation aid (and to alert us) if the mooring should break away prematurely. The cable is standard 0.48-cm nylon-jacketed steel wire, which is widely used in mooring applications.

The RPP is attached in-line to the mooring by means of two bridles below the top cluster of flotation balls. The power module is attached to the mooring 30 m below the transducer to provide vibration isolation. An umbilical cord connects the two electrically. It consists of two 14-gauge conductor leads protected mechanically (e.g., against fish bites) by means of a flexible stainless-steel conduit that is readily clamped to the mooring wire with nylon tiewraps. An integral electromechanical cable had been considered, but the high cost of a custom-made cable could not be justified. (Such a cable would also be very stiff and awkward to handle.) An EGG BACS acoustic release is located at the lower end of the cable. The mooring is attached to three railroad wheels weighing 900 kg by means of 10 m of 1.9-cm nylon line (for shock absorption) and 2 m of 1.2-cm chain.

It is instructive to estimate the expected sound pressure level as a function of distance. The acoustic energy loses its intensity due to cylindrical spreading and absorption. The sound pressure level (SPL) in decibels can be modeled (Urick 1964; Webb and Tucker 1969) as

$$SPL = SL - 10 \log_{10} r_t - 10 \log_{10} r - \alpha r,$$

where r and r_t are measured in meters (r_t is the transition range from spherical to cylindrical spreading and is assumed to be 3 km), α is the attenuation coefficient [=0.6 dB (100 km)$^{-1}$; Clay and Medwin 1977], and SL is the source level. Figure 6 shows SPL for two source levels: 196 dB (upper curve) and 176 dB re 1 μPa @ 1 m (lower curve). The horizontal lines indicate typical ambient noise levels for various wind speeds (Wenz 1962). For distances less than about 500 km, most of the signal loss is due to spreading (represented by the dashed line with slope of $1/r$). At greater distances the attenuation of sound becomes the limiting factor. By increasing the power 20 dB from 176 to 196

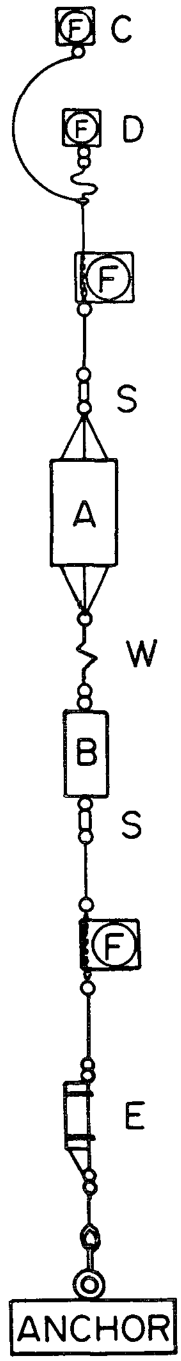

FIG. 5. Schematic drawing of RPP mooring. The wire is standard nylon-jacketed (size) steel cable that is widely used in mooring applications. From top to bottom: ARGOS beacon (C) in glass ball (F), radio/flasher (D) in glass ball (F), 20 glass balls of flotation (F), RPP (A), electronics (B), 10 glass balls of flotation (F), acoustic release (E), and anchor. The letter S refers to a swivel shackle.

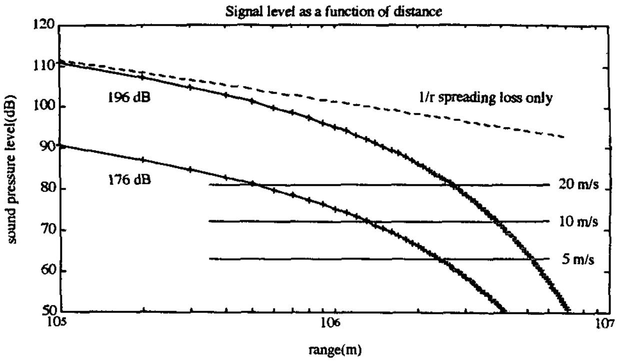

FIG. 6. Computed sound pressure level as a function of distance for two different source levels, 176 and 196 dB re 1 μPa @ 1 m. An attenuation coefficient of 0.6 dB (100 km)$^{-1}$ is assumed. The lines have a $1/r$ slope until about 500 km beyond which attenuation increasingly dominates the spreading losses. Typical ambient noise levels for three different wind speeds indicate the sensitivity of signal detection to weather conditions.

dB, the useful range (defined by the 10 m s^{-1} wind-speed noise cutoff) is increased from 1200 to 3500 km. The spreading losses from the increase in distance are only 5 dB, while the attenuation losses make up the other 15 dB. That a 20-dB increase in power can be accomplished without heavy penalty in battery size is in large measure due to the transducer's 85% conversion efficiency, as noted earlier. The cutoff ranges chosen above are based on 0-dB signal-to-noise ratio. In fact, the signals can be detected at about −5 dB, giving an additional range of some 800 km. The impact of varying wind speed is enormous: at 5 m s^{-1}, typical of the large subtropical regions of the oceans, an additional 1000 km can be obtained!

If substantially greater ranges are desired, such as for operation across the Pacific Ocean, the best way to achieve this would be to drop the operating frequency to 150–200 Hz where the attenuation coefficient is about 0.4 dB (100 km)$^{-1}$. By primarily increasing its length, the RPP could be modified for operation at these frequencies.

4. The prototype field test

The complete system was moored northwest of Bermuda in April 1990. The performance of the system could be monitored from a shore-connected hydrophone nearby. Unfortunately, no signals were received, so the mooring was retrieved a week later. A low pressure hairline leak in one of the connectors to the power module caused a failure of the electronics. The unit was quickly repaired under warranty and the system was scheduled for launch in August that same summer. However, just before launch it was discovered that the transducer had an internal short that had gone undetected after the first test because we had used a standard ohmmeter instead of a high-voltage insulation tester to check the insulation resistance. Water had entered the unit due to crack(s) in the rubberized epoxy coating that was used to protect the transducer. It was necessary to rebuild the entire piezoelectric assembly, which was then encapsulated in an oil-filled neoprene boot. The disassembly and rebuilding of the transducer were done under warranty at SOC during the winter 1990/91. The RPP was recertified by 1) retesting the unit at SOC to 3500-V, 60-Hz hi-pot test; 2) a 1300-db hydrostatic pressure test at DREA; and 3) an acoustic performance test (including a source-level demonstration to 197 dB re 1 μPa) at the U.S. Navy Seneca Lake acoustic test facility. After completion of the tests, the RPP was redeployed at 1400-m depth at the same site about 150 km northwest of Bermuda. This time the test went very well. Deployment took place on 29 May 1991 from the RV *Cape Hatteras,* and recovery took place on 27 November 1991 from the RV *Weatherbird II.*

Two studies of the RPP transmissions were conducted. In both cases comparisons were made with a WRC moored source that was collocated with the RPP on the same seamount about 2 n mi apart on the sound channel axis. Another WRC source was moored on the sound channel axis southeast of Cape Hatteras about 900 km from Bermuda. The first study was simply to monitor the sources from a hydrophone off Bermuda using the filter-signal detection electronics from a RAFOS float. The float receiver is optimized to detect the signal and its arrival time. It cannot measure signal strength, but it does give a measure of the quality or phase stability of the signal. (Recall that the frequency increases linearly with time.) The microprocessor is programmed to conduct a continuous quadrature correlation with the preceding 80 s of the incoming signal. The time (within the preprogrammed 25-min listening window) at which the phase of the preceding 80 s best matches the reference pattern is judged to be the signal time of arrival. The correlation is performed as an exclusive-or and sum operation on 800 bits where each bit describes the phase (+/−) of the incoming signal (after band shifting to low frequency, in this case homodyning) sampled ten times per second (Rossby et al. 1986). A typical correlation height when the phase is random is about |115|; the maximum possible (perfect match) is |400| (after subtracting 400, the mean value for a random input). Figure 7 shows the histogram of correlation heights for signals from the RPP and the other two WRC sound sources. They show that the two sources on the seamount exhibit very similar performance, while the source 900 km away shows some loss of signals with high correlations (but the performance is still very good). The fourth panel shows the percent signals that have the correct arrival time. On two separate occasions a spectrum analyzer was used to make a direct comparison of the sound pressure

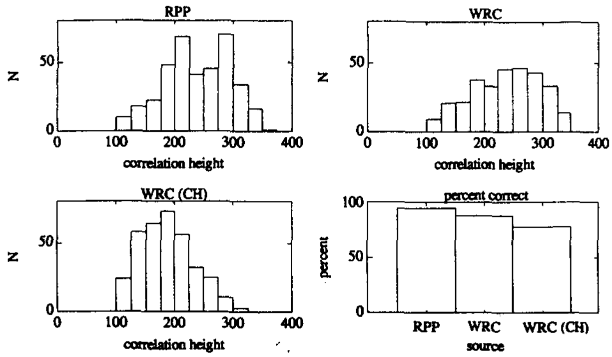

FIG. 7. Correlation heights for signals received at Bermuda from the RPP (top left), the collocated WRC (top right), and the WRC source east-southeast of Cape Hatteras at a distance of about 900 km (lower left). The lower right panel shows the percent signals detected with the correct arrival time.

levels from the RPP and WRC source on the seamount. The differences were 17 and 22 dB, respectively. Since the transmissions were 30 min apart, and the sources are about 2 n mi (=3.7 km) apart, one should not take these numbers too literally, but they are consistent with the design objectives.

The other study was done with a RAFOS float that was released northwest of the Azores at a distance of 2755 km from the RPP and collocated source. The float equilibrated on the sound channel axis. The float was programmed to operate for 45 days, after which it surfaces and telemeters the data to Argos. For data compression reasons, the correlation height is reduced to two bits of information. A 0 means very poor, a 4 very good; however, past experience with RAFOS float data suggests that the quality indicator (QI) is less useful than whether or not the pattern of time of arrivals (TOA) are consistent with reasonable float motion. Both are shown in Fig. 8. The top panel shows the TOAs from the RPP (*) and WRC (+) sources, and the bottom panel shows the corresponding QIs. As expected, at these distances the 20-dB difference in source level is significant. The signals from the RPP are detected correctly 93% of the time, and 17% of the time for the WRC source.

The mooring was recovered on 27 November. The RPP and the power module were in excellent condition with virtually no evidence of corrosion, either electrochemical or due to induced stray currents between the power module and the transducer.

In summary, the resonant pipe projector has performed according to design specifications quite satisfactorily. We believe it is ready for basinwide applications involving long-range acoustic navigation, and for areas where the deep sound channel is absent during the winter half of the year such as the subpolar gyres.

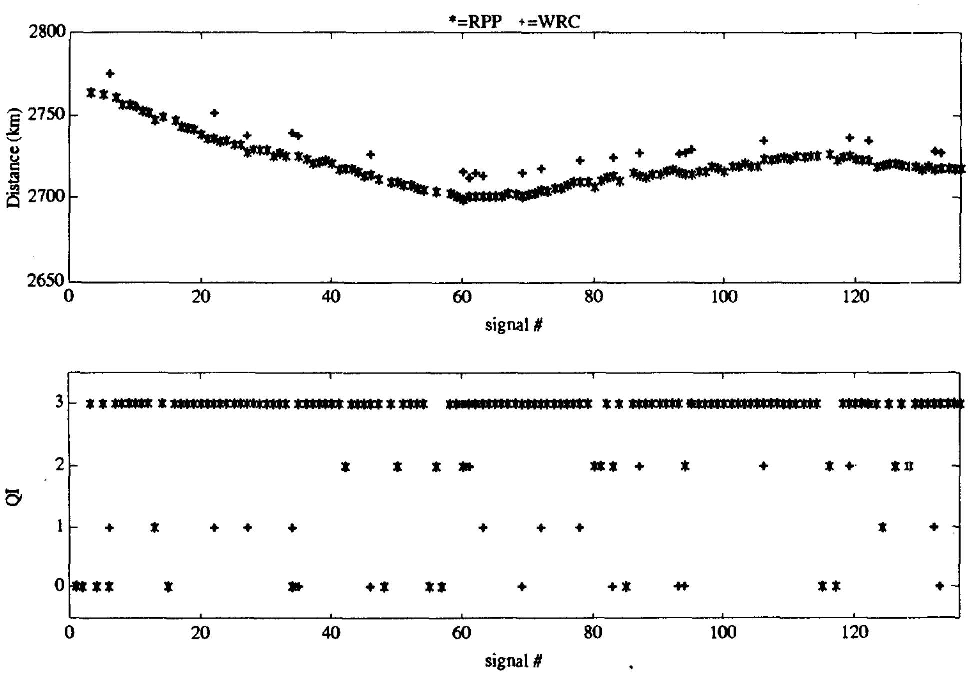

FIG. 8. The top panel shows the RAFOS float distance from the RPP (*) and WRC (+) sources starting at 2755 km. The bottom panel shows the corresponding QI for the two sound sources. The RPP is heard 93% of the time, usually with high QI values; the WRC source is heard 17% of the time.

The RPP is also advantageous for operations where the ambient noise conditions are exceptionally high, such as along the major storm tracks of the North Atlantic.

Acknowledgments. We particularly wish to thank Mr. Linas Siurna at SOC, who provided much technical and logistical support throughout this development program. Dr. E. Carter, Jr., played an important role in this project for bringing Sparton of Canada to our attention! We wish to thank Mr. Tom Orvosh and Mr. John Kemp for the mooring operations, which were handled very smoothly. We are grateful to Dr. R. Watts for detecting the malfunction in the RPP shortly before it was to be moored! We thank the captain and crews of the RV *Cape Hatteras* and RV *Weatherbird II* for their generous and professional assistance during the mooring operations. We also want to thank Dr. Amy Bower for launching a RAFOS float near the Azores and Mr. Joe Cowdrick and his colleagues for operating the shore-based receiver. This work was supported by NSF Grant OCE 87-16924, which is gratefully acknowledged.

REFERENCES

Armstrong, B. A., and G. W. McMahon, 1984: Discussion of the finite-element modeling and performance of ring-shell projectors. IEEE Proc. 131, Part F, 3, 275–279.

Clay, C. S., and H. Medwin, 1977: *Acoustical Oceanography.* Wiley-Interscience, 544 pp.

Ellis, J. W., B. L. Fanning, and G. W. McMahon, 1991: Development of a resonant pipe projector. *Power Transducers and Ultrasonics,* B. F. Harmonic, O. B. Wilson, and J. N. Decarpigny, Eds., Springer-Verlag.

Fanning, B. L., G. W. McMahon, and D. D. Prentiss, 1987: A vented resonant-pipe projector. Proc. Oceans 87 IEEE Conf., **1,** 146–149.

Lee, J. B., 1974: Low-frequency resonant-tube projector for underwater sound. Proc. Oceans 74 IEEE Conf., **2,** 10–15.

Rossby, T., D. Dorson, and J. Fontaine, 1986: The RAFOS system. *J. Atmos. Oceanic Technol.,* **3,** 672–679.

Urick, R. J., 1967: *Principles of Underwater Sound for Engineers.* McGraw-Hill, 342 pp.

Webb, D. C., 1977: SOFAR floats for POLYMODE. Proc. Oceans '77 MTS-IEEE Conf., **2,** 44B–1:5.

——, and M. J. Tucker, 1970: Transmission characteristics of the SOFAR channel. *J. Acoust. Soc. Am.,* **48,** 767–769.

Wenz, G. M., 1962: Acoustic ambient noise in the ocean: Spectra and sources. *J. Acoust. Soc. Am.,* **34,** 1936–1956.

WOCE Implementation Plan, Report 1., 1989: U.S. WOCE Office, Texas A&M University, College Station, TX.